Spectroscopy-based isotopic ($\delta^{13}C$) analysis for high spatial resolution of carbon exchange in the rhizosphere

James J. Moran[1, 2]*, Timothy J. Linley[1], Camille N. Makarem[3], James F. Kelly[3], Eric D. Wilcox Freeburg[1], Daniel M. Cleary[1], M. Lizabeth Alexander[1], and Jason M. Kriesel[3]

[1] Pacific Northwest National Laboratory
[2] Washington State University, Department of Crop and Soil Science, Pullman, WA
[3] Opto-Knowledge Systems, Inc., Torrance, CA

* Correspondence: James Moran; PO Box 999, MSIN K8-91; Richland, WA 99352; james.moran@pnnl.gov

Conflicts of Interest: The authors declare no conflict of interest. The funders had no role in the design of the study; in the collection, analyses, or interpretation of data; in the writing of the manuscript, or in the decision to publish the results.

Funding: System development and testing of the approach was funded by the US Department of Energy (DOE) Office of Biological and Environmental Research by both the Small Business Technology Transfer program, Grant DE-SC0018488 (PI: J. Kriesel) and the Early Career Research Award program (PI: J. Moran). Support for this research was also provided by the Great Lakes Bioenergy Research Center, U.S. Department of Energy, Office of Science, Office of Biological and Environmental Research (Awards DE-SC0018409 and DE-FC02-07ER64494), by the National Science Foundation Long-term Ecological Research Program (DEB 1637653) at the Kellogg Biological Station, and by Michigan State University AgBioResearch. A portion of this research was performed on a project award from the Environmental Molecular Sciences Laboratory, a DOE Office of Science User Facility sponsored by the Biological and Environmental Research program under contract number DE-AC05-76RL01830.

Acknowledgments: The authors thank Matt Peterson and Elizabeth Denis for assistance in collecting IRMS derived sample points. We thank Nathan Johnson for assistance with figure development. We also thank Phil Robertson and Stacey VanderWulp for assistance in collecting soil from the Kellogg Biological Station for use in this experiment.

Spectroscopy-based isotopic ($\delta^{13}C$) analysis for high spatial resolution of carbon exchange in the rhizosphere

Abstract: The rhizosphere is a highly dynamic zone bridging plant roots with needed nutrient resources in soil. While the rhizosphere may be small, it has a disproportionally large impact on plant success and biomass production. A suite of rhizosphere-hosted microbial and geochemical interactions facilitate nutrient acquisition by plant roots, and, in turn, the roots stimulate these processes by supplying organic carbon into the rhizosphere. The small physical dimensions of the rhizosphere, however, can constrain efforts to elucidate key carbon exchange processes and their spatial extent and localization. We present a method for spatially resolved $\delta^{13}C$ analysis of rhizosphere samples by coupling laser ablation (LA) sampling with isotopic analysis using capillary absorption spectroscopy (CAS) which differs from conventional mass spectrometer (MS) approaches. The CAS system has high sensitivity (requires fewer nanomoles of CO_2 per analysis) than comparable MS systems, which enables reduced sample size requirements to thereby improve spatial resolution (from 25μm to as low as a projected 5 μm spatial resolution). We demonstrate the utility of CAS using rhizosphere samples from switchgrass plants exposed to $^{13}CO_2$. This technique will provide a capability for tracking the extent and spatial distribution of root exudate into the rhizosphere at highly detailed spatial scales.

Keywords: spatially resolved stable isotope analysis; root exudate; capillary absorption spectroscopy; laser ablation; carbon isotope

1. Introduction

The rhizosphere is defined as the thin layer of soil surrounding and directly impacted by a plant root [1, 2]. This zone is spatially constrained but supports robust biogeochemical processing with implications for nutrient acquisition, pathogen protection, desiccation resistance, and other soil processes [3-6]. The strong link between effective rhizosphere processes and resulting plant health has important implications

for plant productivity in both natural and agricultural systems. Thus, active rhizosphere management to stimulate beneficial interactions is emerging as a focus area for supporting sustainable agriculture [7-9]. The central driver of plant-stimulated rhizosphere processes is the release of a suite of organic carbon compounds, collectively termed rhizodeposits, by plants and their roots [10]. Quantities of organic carbon released varies by plant type and growth conditions but can constitute a large proportion of net photosynthetic product and can locally alleviate typical carbon limitation in soil ecosystems by suppling a bioavailable carbon source to rhizosphere microbes [11-14]. A class of rhizodeposit released from roots is root exudates, which are known to include both organic carbon and signaling compounds to help shape rhizosphere microbial communities and their functions [15-19].

The wide range of activities performed within the rhizosphere and the important role these play in directing overall plant fitness highlights the need for gaining a mechanistic understanding of rhizosphere function. This is complicated, however, by both the fine spatial scale and spatiotemporal heterogeneity of the rhizosphere, and the extent to which this variability directs relevant metabolic and geochemical interactions [20, 21]. Organic carbon availability can be spatially focused in small regions, driving the development of hotspots within the rhizosphere that host high rates of metabolic activity [22].

The central role that root exudates can play in directing rhizosphere processes and their heterogeneous distribution has led to the development of several complementary techniques for spatially tracking the delivery and fate of this carbon in the rhizosphere [23, 24]. For example, soil zymography enables mapping the distribution of enzymes linked to carbon cycling at spatial scales conducive to rhizosphere studies and can help pinpoint hotspots of carbon consumption [25-27]. Planar optode techniques allow for direct assessment and mapping of metabolic processes linked to carbon respiration, namely oxygen consumption and the production of carbon dioxide [28, 29]. Similarly, emergent techniques in laser induced breakdown spectroscopy (LIBS) are enabling fine-scale mapping of carbon within plant tissues and along the root-rhizosphere-soil continuum [30, 31]. While these approaches can provide needed insights to carbon metabolism and localization with the rhizosphere, they don't independently provide direct, spatially-resolved information on where and how much carbon is being released into the rhizosphere.

52 Established methods with radioactive and stable isotope tracers have been used for monitoring the
53 uptake of carbon dioxide through photosynthesis and subsequent transport of the resulting photosynthate
54 into the root system and rhizosphere. Introducing radioactive elements can provide high-sensitivity tracking
55 of carbon flow. For instance, development of carbon-11 tracer (introduced as $^{11}CO_2$) can provide spatial
56 distribution of photosynthate in the rhizosphere and even permit some evaluation of chemical structure of
57 root exudates [32, 33]. However, a very short half-life for carbon-11 (roughly 20 minutes) constrains the
58 timing between sample collection and analysis and prohibits studies in larger plants where transport time
59 may coincide with large decay in signal. The use of carbon-14 radiocarbon tracers is more widespread and
60 can provide quantified mapping of photosynthate into the rhizosphere [34-37]. Perceived challenges in
61 applying radiocarbon tracers can limit this application, however, and may prohibit additional parallel
62 analysis out of concerns over radioactivity exposure. In part to avoid these concerns, stable isotope tracers
63 (specifically carbon-13) can provide a tool for tracking photosynthate into the rhizosphere and associated
64 microbial and biochemical pools [38]. When coupled with a nano-scale secondary ion mass spectrometer
65 (NanoSIMS), a carbon-13 tracer can reveal highly detailed distribution of recent photosynthate into plant
66 cells, the rhizosphere, and associated microbial cells [39, 40]. However, this approach can be time-
67 consuming, requires a good deal of sample preparation, and can be challenging to perform effective analysis
68 over mm or larger scales that can be relevant for rhizosphere studies [41].

69 Laser ablation-isotope ratio mass spectrometry (LA-IRMS) provides measurement of carbon-13
70 labeled materials at the 10s μm resolution over samples of multiple cm^2, consistent with typical rhizosphere
71 carbon introduction processes [42-46]. The ultimate spatial resolution in these cases is largely driven by
72 sample handling methods and the sensitivity of the IRMS used for analysis, with increased sensitivity
73 requiring smaller sample sizes which in turn enables more focused laser sampling and enhanced spatial
74 resolution. Recent efforts have sought to maximize LA-IRMS sensitivity by optimizing the delivery of
75 sample to the IRMS combined with improved instrument sensitivity performance [45, 47]. While these
76 approaches are successful, the required analyte focusing steps can limit overall sample throughput and the
77 method is still ultimately constrained by sensitivity of the IRMS measurement platform.

78 Capillary absorption spectroscopy (CAS) is an emerging technique for making carbon-13
79 measurements with orders of magnitude sensitivity improvement compared to IRMS [48]. CAS leverages
80 an optically coated capillary (a hollow wave guide; HWG) to create a high optical fill rate with minimized
81 optical losses within short capillary sections [49, 50]. Different rovibrational transitions linked to specific
82 isotopologues (e.g., $^{13}CO_2$ and $^{12}CO_2$) are targeted with a tunable diode laser (mid-wave infrared
83 wavelength) and absorption is correlated with the isotopic population. The small internal volume of the
84 capillary combined with low operating pressures results in the high overall CAS operational sensitivity,
85 requiring as little as 10s picomoles for isotope analysis of carbon dioxide [48]. CAS has several additional
86 advantages over IRMS including its invulnerability to isobaric interferences, potential for improved
87 measurement sensitivity/smaller sample size requirement, smaller footprint and reduced peripheral
88 instrument support (e.g., lower vacuum and power requirements), and potential for field deployment. Our
89 goal was to build upon the work of Kelly et al. [48] and Kriesel et al. [51] to construct a modified CAS
90 system integrated with a laser ablation sampling device to evaluate the utility of this instrument to provide
91 spatially resolved isotopic measurements along the root-rhizosphere system, using a switchgrass microcosm
92 as a model system to test the application. We present a method and the resulting data from these samples
93 that highlight the potential role LA-CAS may play in future rhizosphere investigations.
94

95 **2. Materials and Methods**

96 *2.1 Sample growth, isotopic labeling, and preparation*

97 To test the effectiveness of the LA-CAS system on rhizosphere samples, we grew switchgrass
98 (*Panicum* virgatum, variety Cave-in-rock [52]) in rhizobox systems (**Figure S1**) following the methods of
99 Ilhardt et al., 2019 [30]. Briefly, we filled the rhizoboxes with a sandy loam Alfisol harvested from the A
100 and upper B soil horizons within established switchgrass plots at the Kellogg Biological Station (Hickory
101 Corners, MI, USA) [53]. We sieved (4 mm) the harvested soil then packed it into the high-density

102 polyethylene rhizoboxes (12.7 cm x 19 cm x 1 cm). We transplanted switchgrass seedlings (germinated in
103 shallow water dishes) into the rhizoboxes and grew the plants in a Conviron (Winnipeg, Manitoba, Canada)
104 walk-in growth chamber (model no. GR48) at 24 °C / 50% relative humidity during the day and 18 °C /
105 40% relative humidity at night (16 hour light / 8 hour dark cycle). After approximately six weeks of growth,
106 we transferred the rhizobox systems into a stable isotope labeling cell which was itself placed within the
107 growth chamber, injected $^{13}CO_2$ (99 atom%, Sigma-Aldrich, St. Louis, Missouri, USA) into the chamber,
108 and continued plant growth for an additional 48 hours to isotopically label plant photosynthate produced
109 during this time. We added additional $^{13}CO_2$ aliquots at approximately four-hour intervals during the
110 daylight growth phase to provide a constant supply of CO_2. We subsampled the root-rhizosphere-soil
111 system by removing one side of the rhizobox to expose the subsurface plant biomass and used a ½" diameter
112 coring device to extract samples while preserving their spatial orientation [44]. We pressed the upper
113 surface of the sample to remove topographical artifacts that could reduce the effectiveness of laser ablation
114 while retaining the sample's 2D spatial orientation, then froze (-80°C) and lyophilized the samples in
115 preparation for analysis.
116

117 *2.2 Sample analysis*

118 2.2.1 Sample selection and laser ablation extraction

119 We sought to compare and evaluate the merits of LA-CAS and LA-IRMS methods and directly
120 compared analyses of the same sample for each type of analysis when possible. This included running
121 parallel, side-by-side transects of the $\delta^{13}C$ spreading perpendicularly from a plant root where a transect
122 performed using LA-CAS was bracketed by data collected using LA-IRMS. To make these measurements,
123 we followed previously described methods [54] for LA-IRMS and adapted the approach to permit LA-
124 CAS. Briefly, we employed a CETAC LSX-500 (now Teledyne CETAC Technologies, Omaha, NE, USA)
125 laser ablation system for imaging and spatially targeting a section of the sample to be analyzed. All sample

126 locations were manually selected by the laser ablation operator but generally arranged to form a linear array
127 of sample points. We adjusted the number of laser ablation pulses incident on the surface of the sample
128 based on the measurement platform (CAS or IRMS) being used and the relative carbon abundance within
129 a targeted area to ensure a reasonable sample size for downstream isotope measurement. Thus, we generally
130 used fewer ablation pulses when sampling for CAS versus IRMS measurement (based on the higher
131 instrument sensitivity of the CAS system) and used fewer ablation pulses for sampling root versus
132 rhizosphere and soil samples (based on the higher carbon abundance in roots versus the surrounding soil
133 (Table 1). The improved sensitivity of the CAS system also enabled use of a smaller ablation spot size
134 compared to IRMS sampling.

135

136 **Table 1: Laser ablation parameters used for sampling**

Measurement approach	LA-IRMS			LA-CAS		
Sample matrix	root	rhizosphere/soil	fishing line	root	rhizosphere/soil	fishing line
Ablation diameter (μm)	50	50	50	25	25	25
Number of ablation shots	1 - 10	80 - 100	8	1 - 2	30	2 - 3
Final sampling pit width (μm)	50	100	50	25	25	25
Ablation frequency (Hz)	20	20	20	20	20	20
Approximate power (mJ)	≤ 9	≤ 9	≤ 9	≤ 9	≤ 9	≤ 9

137

138

139 Particulates released during the ablation process were entrained in a helium carrier stream (10 mL/min)
140 and passed through an alumina micro-combustion reactor heated to 950 °C. The reactor contained nickel
141 and platinum wire as catalysts and was supplied with a slow oxygen bleed to help maintain oxidizing
142 conditions. The resulting CO_2 was transported by the helium carrier gas into a capillary cryotrap immersed
143 in liquid nitrogen to focus the CO_2. Following trapping (generally for a total duration of one minute), we
144 reduced the helium carrier flow to 1 mL/min, melted the trap, and permitted the CO_2 to flow into the detector
145 of the IRMS or CAS system.

146

147 2.2.2 Isotopic measurement using CAS

148 The basic arrangement for the CAS is shown in **Figure 1**. The laser ablation unit produced particulates
149 that were combusted to CO_2 within the combustion reactor (see 2.2.1 and [54]). Soil, root samples, and
150 standards were ablated by a single point method consisting of 1-30 pulses depending on the material (Table
151 1) to maintain ≤ 10% absorbance to prevent detector saturation. The laser ablation beam was set to 25 μm
152 spot diameter, 100% power, and frequency of 20 Hz. Previous work using this laser ablation system showed
153 the resulting particle sizes produced by ablation with these parameters were sized well below one micron,
154 ensuring complete and quantitative combustion into CO_2 prior to cryotrapping [54]. The CO_2 was carried
155 to the CAS by helium (He) gas at a flow rate of 10 mL/min and required approximately 12-13 sec to reach
156 the fiber after the ablation pulse on a flow-through basis. The timing of the pulse was used to manually
157 toggle the three-way micro-fluid valve from a venting to a delivery position and direct the gases into a
158 second section of capillary tubing immersed in liquid nitrogen to cryo-trap and concentrate the CO_2. The
159 timing of this process and duration of the valve in the delivery position (~ 5 sec) were optimized to capture
160 as much CO_2 as possible while minimizing the amount of He injected into the CAS. Once the sample CO_2
161 was trapped, incoming carrier gas was deflected to the vent and the trapped CO_2 was allowed to warm and
162 expand into the CAS hollow wave guide (HWG). The HWG measured 2.0 m in length with an internal
163 diameter of 500 μm and had a dielectric (AgI) internal coating to optimize transmission of wavelengths
164 approximating 4.35 μm [55]. The total internal volume of the HWG was 0.393 cm^3. The ends of the HWG
165 were fitted with sealed BaF2 windows cantered at an angle of ~ 5° to reduce reflective feedback to the laser.
166 The sample pathway from the laser ablation system to the CAS fiber is depicted in green (**Figure 1**).
167
168

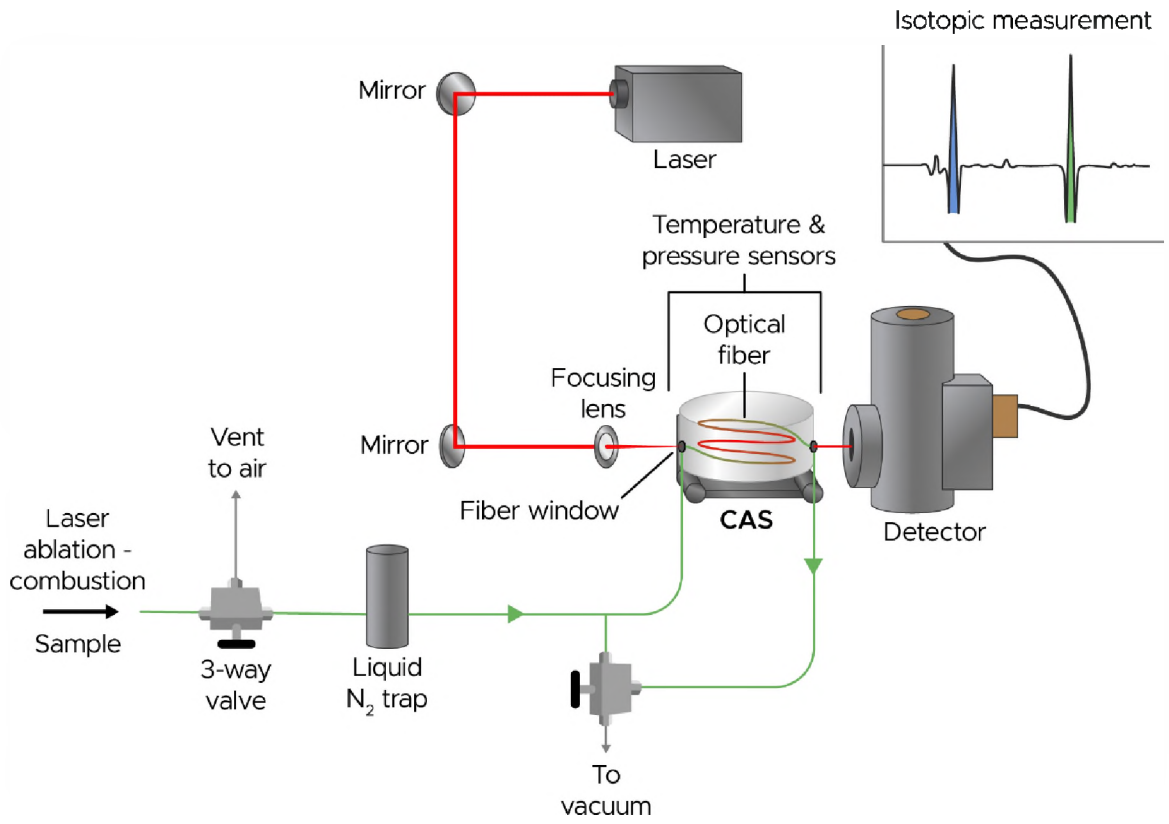

Figure 1: Sample derived CO_2 (green flow path) is cryofocused using a liquid nitrogen trap then introduced into an evacuated CAS HWG. A modulated incident light source (red path) is focused into the HWG and, upon exciting, a detector is used to monitor absorbance within the HWG which is then transformed to independent quantification of CO_2 isotopologues.

Prior to cryo-trapping the internal pressure in the CAS was reduced to < 8 mTorr with a vacuum pump (Hi CUBE Eco 80, Pfeiffer Vacuum Technology AG, Asslar, Germany) to remove residual CO_2 in the system. During laser ablation, He entered the CAS generating positive pressure of ~ 250-300 Torr as the CO_2 from the ablated material entered the cryo-trap. Once trapping was completed, the pressure within the fiber was again reduced to < 8 mTorr prior to closing a 3-way valve downstream of the fiber leading to the vacuum line. At this time, the trapping capillary was removed from the liquid nitrogen allowing CO_2 to

181 enter the system under negative pressure. The absorbance bands of CO_2 containing the optical transitions
182 for ^{12}C and ^{13}C were recorded, the peaks from multiple measurement cycles were averaged using a second
183 derivative (2f) demodulation. The central peak area under the 2f peaks were associated with the respective
184 ^{13}C and ^{12}C transitions to estimate a raw $^{13}C/^{12}C$ ratio of the sample. These relative values were then
185 anchored to an in-house standard calibrated by IRMS. Once the data were recorded, the system was flushed
186 with He to remove the sample CO_2 then returned to vacuum conditions for the next sample. We performed
187 analysis on a half dozen samples and used a series of point ablations targeting the root and then
188 perpendicular across the rhizosphere for each sample.
189
190 The electronic instrumentation used to measure CO_2 within the HWG is shown in Figure S2. The laser
191 beam for the HWG was supplied by a distributed feedback interband cascade laser (Nanoplus 4355 nm)
192 and diode controller (Arroyo Instruments 6305). A positive linear ramp current (~ 45 nA) was applied to
193 the laser with a digital signal oscillator (DSO) (Agilent 33250A) at a frequency and amplitude of 20 Hz and
194 140 mV, respectively. This enabled the laser emission to rapidly ramp across the wavenumbers
195 corresponding to the targeted CO_2 spectroscopy transitions for $^{12}CO_2$ and $^{13}CO_2$ used for analysis
196 (nominally 2295.85 and 2296.05 cm^{-1} respectively). The incident light was directed to the HWG using two
197 flat mirrors (as shown in **Figure 1**) to co-align the collimated laser beam to the input axis of the HWG and
198 using a focusing lens (focal distance = 70 mm) to couple into the 0.5 mm diameter HWG. The output from
199 the HWG was captured with an InSb photodetector (Cincinnati Electronics SDD-7854-S1-05M) which was
200 cooled with liquid nitrogen with the output connected to a digital signal processing lock-in amplifier (Lock-
201 In Amplifier, Perkin Elmer 7280). A diplexer, positioned in-line after the photodetector, split the 2f (or
202 second derivative) and direct absorbance signals and directed them to an oscilloscope (Tektronix TBS
203 1202B; for manual observation), respectively. The analog linear ramp generated by DSO was modulated at
204 a frequency of 58 kHz and amplitude of 350 mV using the internal oscillator of the lock-in amplifier, then
205 attenuated at 30 db (HP 355D VHF Attenuator) to reduce any transient signal or static pickup from
206 overpowering the laser controller. An appropriately attenuated frequency modulation (FM) signal directed

to an inline diplexer was added to a slower, quasi-dc ramp signal and the combined signal passed to a second inline diplexer that added the dc signal from the laser ramp, which passed the combined signal to the laser controller. The FM-to-AM signal was recovered and demodulated by the lock-in-amplifier, then directed to the second channel of oscilloscope as the 2f output.

The separate ^{12}C and ^{13}C peaks measured for making an isotopic assessment are linked to different rovibrational transitions in carbon dioxide (**Figure 2**). The proximity of these two peaks makes them ideal for the needed isotope measurement because it reduces laser scanning time and distance (minimal wavenumber offset between the two relevant peaks). However, one implication of using these transitions is that the two isotopolgue peaks have different calibration factors. To ensure the accuracy of our measurements where isotopic calibration was desired, we used an in-house fishing line standard (sampled before and after a set of rhizosphere samples) for calibrating all the isotopic measurements performed with the CAS system. In short, we took the simple quotient of the measured ^{13}C and ^{12}C peak areas (where $^{13}C/^{12}C$ = R, or the isotopic ratio) for the fishing line standard and divided this by the known $^{13}C/^{12}C$ (R) for the fishing line (0.0109263; [54]) to establish a daily correction factor (equation 1).

$$\frac{R_{CAS\ measurement}}{R_{fishing\ line\ standard}} = correction\ factor \qquad \text{(equation 1)}$$

The raw $^{13}C/^{12}C$ for each sample peak was then multiplied by this correction factor to determine the sample R which is then converted to delta (δ) notation using equation 2.

2.2.3 Isotopic measurements using IRMS

Carbon dioxide generated from the laser ablation sampling and combustion was passed through a Nafion (Chemours Company, Wilmington, DE, USA) containing water drier and directly into a 20-22 IRMS (Sercon Limited, Cheshire, U.K.). We used a small length of 15-pound test monofilament nylon

230 fishing line as an isotopic standard ($\delta^{13}C$= -27.71‰, [54]) for data calibration and report all isotope
231 measurements using delta (δ) notation (equation 1) in per mil (‰) units where:

$$\delta^{13}C = \left[\frac{R_{sample}}{R_{standard}} - 1\right] \times 1000 \qquad \text{(equation 2)}$$

232

233 and R_{sample} and $R_{standard}$ represent the isotope ratio ($^{13}C/^{12}C$) of the sample and Vienna Pee Dee Belemnite
234 (VPDB; 0.0112372) respectively. In a subset of analyses, we report $\Delta^{13}C$ which we use to indicate the
235 isotopic difference between two measurements.

236

237

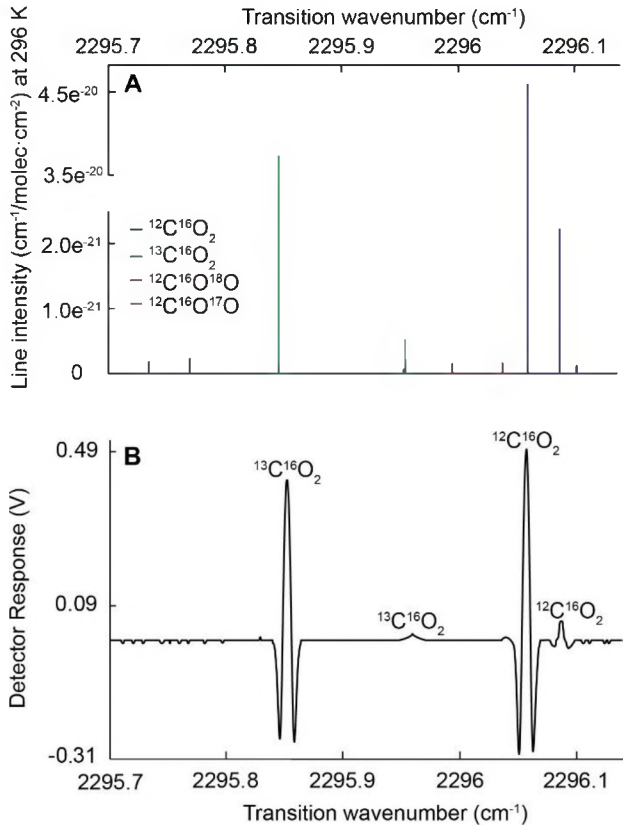

238

239 **Figure 2:** A) Rovibrational absorption peaks within the targeted analysis range based on HITRAN database
240 [56]. We identified a spectroscopic location where isolated $^{13}CO_2$ and $^{12}CO_2$ isotopologues were present in

close (wavenumber) proximity and had similar intensities for laser-based selection. B) We recorded the absorbance in this region and compared the 2f conversion data (B) of peaks associated with the ^{12}C and ^{13}C isotopologues and used this comparison as a basis for $\delta^{13}C$ quantification.

3. Results

3.1 Initial isotopic measurement

To perform the initial evaluation of LA-CAS, we selected a section of root and rhizosphere and employed a linear ablation pattern to compare the isotopic enrichment in the plant roots, the immediately adjacent rhizosphere, and the more distal rhizosphere located ~ 500 μm from the root edge (**Figure 3**). In this initial example, we did not perform cryogenic trapping of CO_2 but performed an isotopic measurement as sample was continually ablated and the resulting CO_2 passed through the CAS fiber. We report $\Delta^{13}C$ as a relative comparison between the sampling locations and leveraged the distal rhizosphere sampling location as a basis for normalization (i.e., reported isotope data are relative to the distal rhizosphere sample). As expected, ^{13}C content increased from the distal to proximal rhizosphere followed by an incremental increase in ^{13}C in the plant root itself.

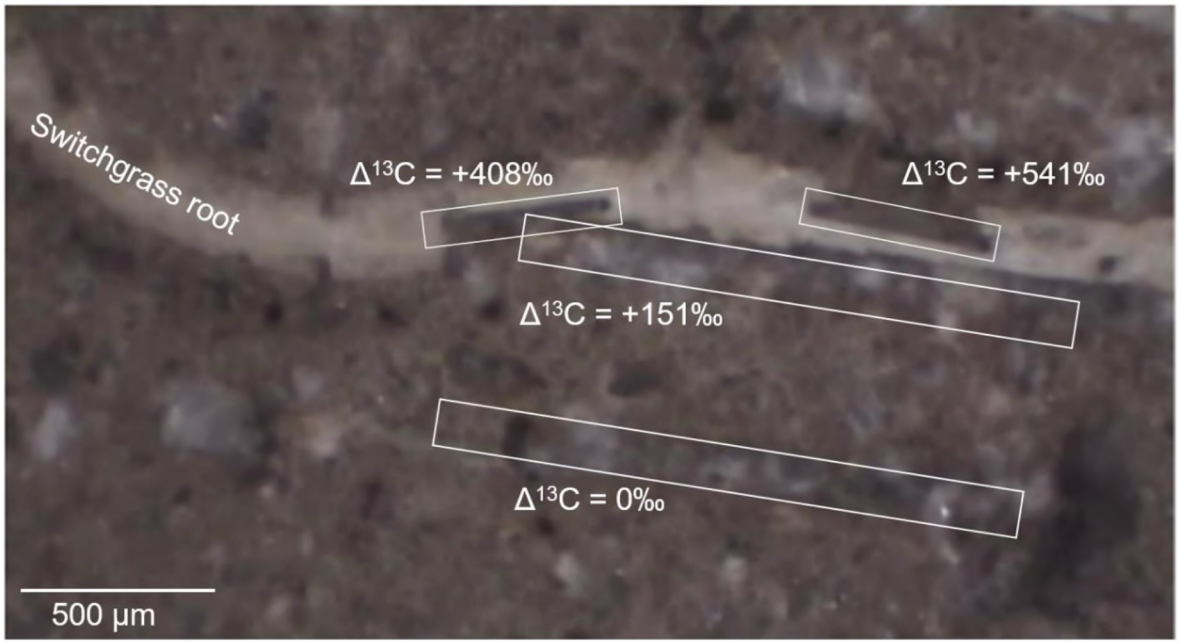

Figure 3: LA-CAS was performed on a plant root and within "proximal" and "distal" rhizosphere sections. A root is seen traversing the field of view from left to right in this image with the region outside the root composed of soil harvested from the rhizobox. Here, continuous ablation of material (outlined by the four rectangular boxes in the image) provided a flow of sample-derived CO_2 which was isotopically characterized by CAS. The results showed highest levels of ^{13}C tracer in the root material with sequentially decreasing levels in the proximal and distal rhizosphere.

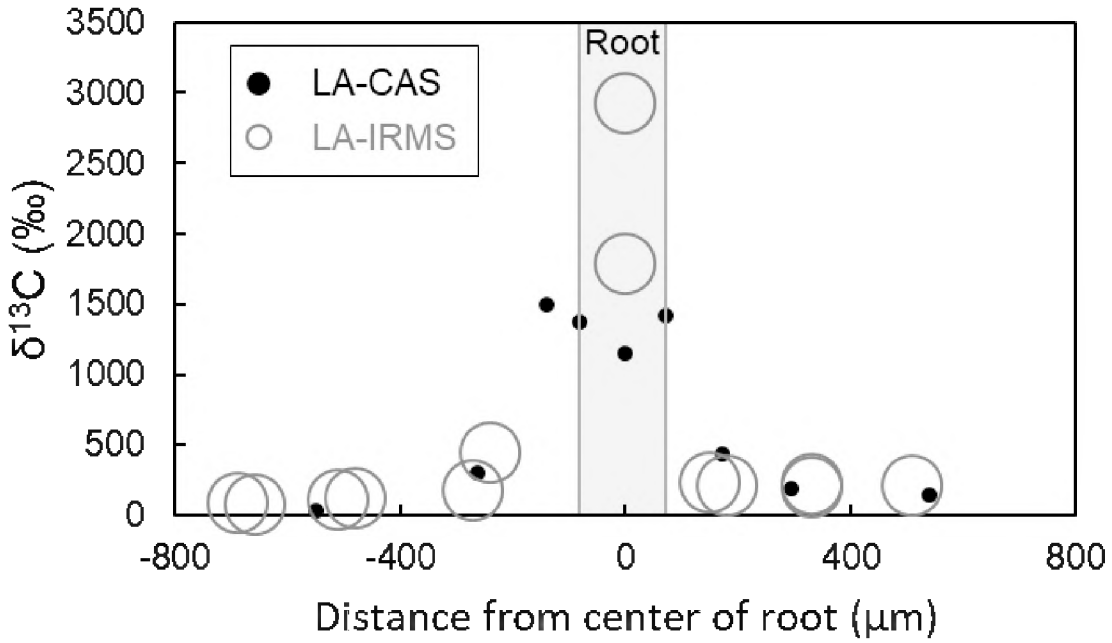

Figure 4: A comparison of measured $\delta^{13}C$ using the LA-CAS and LA-IRMS techniques. Data was collected from slightly different sections of the same sample and plotted in relation to distance from the same plant root. The data points are plotted roughly at scale where the laser ablation pit diameter resulting from LA-IRMS analysis is roughly 100 μm in diameter while that associated with LA-CAS analysis was roughly 25 μm in diameter. Thus, from a surface area perspective, roughly 16 times more material was harvested for IRMS (versus CAS) analysis.

3.2 Comparison of LA-CAS with LA-IRMS

To directly compare LA-CAS and LA-IRMS performance on identical samples, we used cryofocusing for both systems and performed $\delta^{13}C$ analyses at distinct point locations in the sample. Given the destructive sampling nature of laser ablation, we were unable to use the exact same location for each analysis type, but instead, spatially bracketed a series of analyses along parallel paths. Results **(Figure 4)** showed similar trends of decreasing $\delta^{13}C$ at increasing distances from the root where measurements were performed from directly on the root to over 0.5 mm away from the root surface. We performed LA-CAS on six samples and while, given spatial heterogeneity of rhizosphere these may not be considered strict replicates, each of the

280 results were generally consistent and showed decreasing $\delta^{13}C$ at increasing distance from the root surface
281 into the rhizosphere. The LA-CAS results tend to saturate with rich $\delta^{13}C$ regions such that at extremely high
282 ^{13}C levels it may be preferred to integrate areas of direct absorbance (vs 2f conversion).

283 **4. Discussion**

284 We observed consistency between LA-CAS and LA-IRMS results where, in each case, measured $\delta^{13}C$
285 decreased with increasing distance from the plant root, helping highlight previously documented decline in
286 exudation-derived carbon away from a plant root [34, 36, 44]. Importantly, the observed amplitude of the
287 $\delta^{13}C$ spike in both measurement types was similar such that estimates of root exudate based on the data in
288 each case would be nearly identical. There were, however, some distinctions between the measurements
289 largely linked to the improved sensitivity of CAS versus IRMS. This sensitivity enabled measurement of
290 less total carbon and correlated to fewer laser ablation shots and smaller ablation spot sizes for LA-CAS
291 versus LA-IRMS and had implications for 1) the ultimate spatial resolution of the analysis and 2) potential
292 subsequent analyses of the sample.

293 First, the smaller sample spot sizes used in LA-CAS can directly correlate to improved spatial
294 resolution of $\delta^{13}C$ measurements. One instance of this is potentially displayed as a feature in the data
295 collected from sampling of the plant root itself. Sample requirements for LA-IRMS led to 100 μm spot
296 sizes which limited the number of distinct sampling locations over the root surface. In contrast, LA-CAS
297 used 25 μm spot sizes and multiple distinct measurements were performed across the root. A pattern that
298 emerged in many of the LA-CAS transects over the root included the feature observed here (**Figure 4**),
299 where there was a discernable decrease in the measured $\delta^{13}C$ in the center portion of the root. While we do
300 not yet understand the reason for this phenomenon, it is possible that the spatial specificity of the
301 measurement was able to capture either 1) a shift in $\delta^{13}C$ associated with morphological structures (likely
302 root vasculature where cells associated with water uptake may have less ^{13}C than those associated with
303 transport of fresh photosynthate) within the root or 2) the $\delta^{13}C$ of root exudate was more isotopically
304 enriched than the $\delta^{13}C$ of the root itself and the measurements taken closer to the root edge captured a higher

305 proportion of exudate material then the measurement in the center of the root. Given the short nature of the
306 applied $^{13}CO_2$ pulse (only two diurnal cycles), it is likely that the $\delta^{13}C$ of the root cells themselves contain
307 less ^{13}C than that of any photosynthate the roots may be transporting given that the root biomass was likely
308 synthesized prior to the tracer application (based on the root size and associated presumed age). While the
309 exact phenomenon observed here is challenging to identify, related studies have documented the important
310 role that small scale spatial heterogeneity can play as a key driver of hotspot formation, activity, and
311 duration [22, 57].

312 Secondly, smaller ablation pits were produced in the LA-CAS analyses which resulted in less sample
313 removal (**Figure 5**). Laser ablation is a destructive technique by definition since sample is physically
314 removed in the process. However, this impact is largely contained with the ablation pit and evidence
315 indicates that further analytical techniques such as DNA extractions and sequencing [58] and elemental
316 analysis [30] can be performed on a single sample following LA analysis. Further, it is important to note
317 that the sample preparation needed for LA-CAS involves only collecting and drying the sample with no
318 addition of contaminants or other factors that would impede metaproteomic [59], lipidomic [60],
319 metabolomic [61], combined multi-omic [62], or other types of analysis that could be integrated with the
320 $\delta^{13}C$/root exudation information provided by LA-CAS. Thus, the smaller pit sizes resulting from LA-CAS
321 can help preserve sample material that would otherwise be lost (i.e., by performing LA-IRMS analysis) and
322 thereby facilitate collection of complementary data that would further refine the analysis of such complex
323 systems. With the improved sensitivity of CAS based analysis it would be possible to "throttle" sample
324 intake with fewer ablation pulses to help the CAS analyzer stay in its linear range. It is important to reiterate
325 the tight metabolic connectivity between root exudates and the resulting rhizosphere microbiome where
326 changes in root exudation have been linked to shifts in microbiome community structure [16] and resulting
327 enzymatic activity [63]. Thus, preserving as much sample material as possible for subsequential analysis
328 of microbial and biochemical analysis can be critical for enabling comprehensive understanding of
329 connected biogeochemical processes within rhizosphere.

330

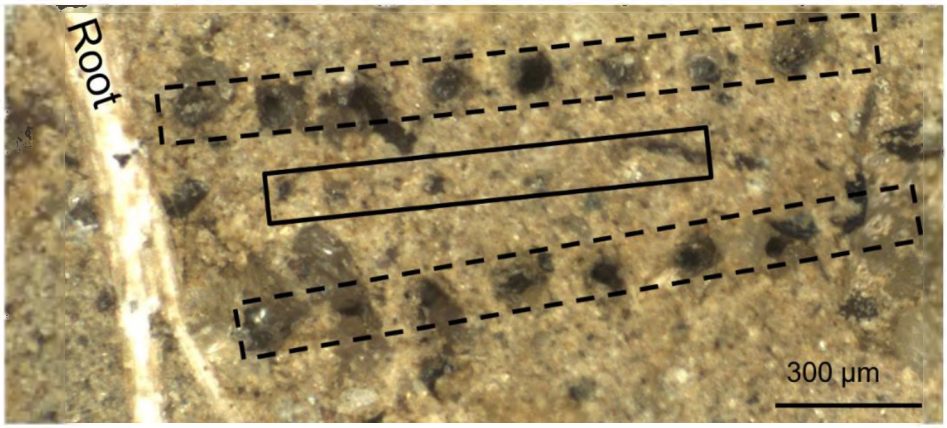

Figure 5: A visual comparison of laser ablation pits resulting from sampling for either IRMS (dashed box) or CAS (solid box). A root passes vertically through the left side of this image with discreet laser ablation points aligned perpendicular to and progressing across the rhizosphere to the right of the root surface. The higher sample requirement for IRMS analysis resulted in increased sample removal (~100 µm diameter ablation pits) versus those needed for CAS analysis (~25 µm diameter ablation pits), potentially limiting the types or fidelity of subsequent sample analyses.

5. Conclusions

Looking forward, there is growing acknowledgement of the central role of soil in preserving overall ecosystem habitability [64] which is fostering an emphasis on understanding key processes within soil that have a direct link to various agricultural outcomes, soil sequestration of carbon, and a wide variety of other functions. Root exudation (as a form of rhizodepositon) is not only a major pathway for the introduction of carbon into soils [65, 66], but also forms a foundational support for microbial processes intrinsically linked to overall soil carbon cycling, with direct implications for controls on plant and ecosystem health. Yet, introduction of carbon through root exudation is spatiotemporally heterogeneous with hotspots of entry changing in response to a wide range of inputs. Here, we demonstrate the LA-CAS method coupled with the use of a $^{13}CO_2$ tracer as an effective tool for performing spatially resolved $\delta^{13}C$ analysis with the goal of enabling quantitative tracking of carbon entry into rhizosphere and, subsequently, into soil. This method provides improved spatial resolution (up to 25 µm for analysis of rhizosphere and soil as used here) over

existing approaches such as LA-IRMS while remaining straightforward in application and without requiring extensive sample preparation. Further, LA-CAS is conducive to subsequent analyses of a sample by a wide range of additional tools to help capture the breadth of microbial and geochemical processes that ultimately control the fate of this carbon.

References

[1] A. Hartmann, M. Rothballer, M. Schmid, Lorenz Hiltner, a pioneer in rhizosphere microbial ecology and soil bacteriology research, Plant Soil 312(1-2) (2008) 7-14.
[2] L.M. York, A. Carminati, S.J. Mooney, K. Ritz, M.J. Bennett, The holistic rhizosphere: integrating zones, processes, and semantics in the soil influenced by roots, Journal of Experimental Botany 67(12) (2016) 3629-3643.
[3] H.P. Bais, T.L. Weir, L.G. Perry, S. Gilroy, J.M. Vivanco, The Role of Root Exudates in Rhizosphere Interations with Plants and Other Organisms, Annual Review of Plant Biology 57 (2006) 233-266.
[4] H. Lambers, C. Mougel, B. Jaillard, P. Hinsinger, Plant-microbe-soil interactions in the rhizosphere: an evolutionary perspective, Plant Soil 321(1-2) (2009) 83-115.
[5] D.M. Weller, Biological Control of Soilborne Plant Pathogens in the Rhizosphere with Bacteria, Annu Rev Phytopathol 26 (1988) 379-407.
[6] P. Hinsinger, C. Plassard, C.X. Tang, B. Jaillard, Origins of root-mediated pH changes in the rhizosphere and their responses to environmental constraints: A review, Plant Soil 248(1-2) (2003) 43-59.
[7] J. de Vrieze, The Littlest Farmhands, Science 349(6249) (2015) 680-683.
[8] Y.X. Zhang, C. Ruyter-Spira, H.J. Bouwmeester, Engineering the plant rhizosphere, Curr Opin Biotech 32 (2015) 136-142.
[9] P.R. Ryan, Y. Dessaux, L.S. Thomashow, D.M. Weller, Rhizosphere engineering and management for sustainable agriculture, Plant Soil 321(1-2) (2009) 363-383.
[10] D.L. Jones, C. Nguyen, R.D. Finlay, Carbon flow in the rhizosphere: carbon trading at the soil–root interface, Plant Soil 321(1-2) (2009) 5-33.
[11] L. Philippot, J.M. Raaijmakers, P. Lemanceau, W.H. van der Putten, Going back to the roots: the microbial ecology of the rhizosphere, Nat Rev Microbiol 11(11) (2013) 789-99.
[12] Y. Mao, X. Li, E.M. Smyth, A.C. Yannarell, R.I. Mackie, Enrichment of specific bacterial and eukaryotic microbes in the rhizosphere of switchgrass (Panicum virgatum L.) through root exudates, Environ Microbiol Rep 6(3) (2014) 293-306.
[13] C. Nguyen, Rhizodeposition of organic C by plants: mechanisms and controls, Agronomie 23(5-6) (2003) 375-396.
[14] Y. Kuzyakov, G. Domanski, Carbon input by plants into the soil. Review, Journal of Plant Nutrition and Soil Science 163(4) (2000) 421-431.
[15] P.G. Dennis, A.J. Miller, P.R. Hirsch, Are root exudates more important than other sources of rhizodeposits in structuring rhizosphere bacterial communities?, Fems Microbiol Ecol 72(3) (2010) 313-327.
[16] K. Zhalnina, K.B. Louie, Z. Hao, N. Mansoori, U.N. da Rocha, S. Shi, H. Cho, U. Karaoz, D. Loque, B.P. Bowen, M.K. Firestone, T.R. Northen, E.L. Brodie, Dynamic root exudate chemistry and microbial

substrate preferences drive patterns in rhizosphere microbial community assembly, Nature Microbiology 3(4) (2018) 470-480.
[17] T.S. Walker, H.P. Bais, E. Grotewold, J.M. Vivanco, Root exudation and rhizosphere biology, Plant Physiol 132(1) (2003) 44-51.
[18] F.e.Z. Haichar, C. Santaella, T. Heulin, W. Achouak, Root exudates mediated interactions belowground, Soil Biology and Biochemistry 77 (2014) 69-80.
[19] P.A. Bakker, R.L. Berendsen, R.F. Doornbos, P.C. Wintermans, C.M. Pieterse, The rhizosphere revisited: root microbiomics, Front Plant Sci 4 (2013) 165.
[20] D.L. Jones, P. Hinsinger, The rhizosphere: complex by design, Plant Soil 312(1-2) (2008) 1-6.
[21] Z.G. Cardon, D.J. Gage, Resource Exchange in the Rhizosphere: Molecular Tools and the Microbial Perspective, Annual Review of Ecology, Evolution, and Systematics 37(1) (2006) 459-488.
[22] Y. Kuzyakov, E. Blagodatskaya, Microbial hotspots and hot moments in soil: Concept & review, Soil Biology and Biochemistry 83 (2015) 184-199.
[23] E. Oburger, H. Schmidt, New Methods To Unravel Rhizosphere Processes, Trends Plant Sci 21(3) (2016) 243-55.
[24] J. Moran, C. McGrath, Comparison of methods for mapping rhizosphere processes in the context of their surrounding root and soil environments, Biotechniques 71(6) (2021).
[25] M. Spohn, A. Carminati, Y. Kuzyakov, Soil zymography – A novel in situ method for mapping distribution of enzyme activity in soil, Soil Biology and Biochemistry 58 (2013) 275-280.
[26] A. Guber, A. Kraychenko, B.S. Razavi, D. Uteau, S. Peth, E. Blagodatskaya, Y. Kuzyakov, Quantitative soil zymography: Mechanisms, processes of substrate and enzyme diffusion in porous media, Soil Biol Biochem 127 (2018) 156-167.
[27] X.M. Ma, Y. Liu, M. Zarebanadkouki, B.S. Razavi, E. Blagodatskaya, Y. Kuzyakov, Spatiotemporal patterns of enzyme activities in the rhizosphere: effects of plant growth and root morphology, Biology and Fertility of Soils 54(7) (2018) 819-828.
[28] N. Lenzewski, P. Mueller, R.J. Meier, G. Liebsch, K. Jensen, K. Koop-Jakobsen, Dynamics of oxygen and carbon dioxide in rhizospheres of Lobelia dortmanna - a planar optode study of belowground gas exchange between plants and sediment, New Phytol 218(1) (2018) 131-141.
[29] S. Blossfeld, C.M. Schreiber, G. Liebsch, A.J. Kuhn, P. Hinsinger, Quantitative imaging of rhizosphere pH and CO2 dynamics with planar optodes, Ann Bot-London 112(2) (2013) 267-276.
[30] P.D. Ilhardt, J.R. Nuñez, E.H. Denis, J.J. Rosnow, E.J. Krogstad, R.S. Renslow, J.J. Moran, High-resolution elemental mapping of the root-rhizosphere-soil continuum using laser-induced breakdown spectroscopy (LIBS), Soil Biology and Biochemistry 131 (2019) 119-132.
[31] D. Santos, L.C. Nunes, G.G.A. de Carvalho, M.D. Gomes, P.F. de Souza, F.D. Leme, L.G.C. dos Santos, F.J. Krug, Laser-induced breakdown spectroscopy for analysis of plant materials: A review, Spectrochim Acta B 71-72 (2012) 3-13.
[32] L.H. Song, B. Agtuca, M.J. Schueller, S.S. Jurisson, G. Stacey, R.A. Ferrieri, Relationship Between Carbon Mobilization and Root Growth Measured by Carbon-11 Tracer in Arabidopsis Starch Mutants, J Plant Growth Regul 38(1) (2019) 164-179.
[33] M.R. Kiser, C.D. Reid, A.S. Crowell, R.P. Phillips, C.R. Howell, Exploring the transport of plant metabolites using positron emitting radiotracers, Hfsp J 2(4) (2008) 189-204.
[34] D. Sauer, Y. Kuzyakov, K. Stahr, Spatial distribution of root exudates of five plant species as assessed by14C labeling, Journal of Plant Nutrition and Soil Science 169(3) (2006) 360-362.
[35] M. Holz, M. Zarebanadkouki, Y. Kuzyakov, J. Pausch, A. Carminati, Root hairs increase rhizosphere extension and carbon input to soil, Ann Bot-London (2018).
[36] J. Pausch, Y. Kuzyakov, Photoassimilate allocation and dynamics of hotspots in roots visualized by 14C phosphor imaging, Journal of Plant Nutrition and Soil Science 174(1) (2011) 12-19.
[37] Silke Hafner, Guido L.B. Wiesenberg, Ekaterina Stolnikova, Klara Merz, Y. Kuzyakov, Spatial distribution and turnover of root-derived carbon in alfalfa rhizosphere depending on top- and subsoil properties and mycorrhization, Plant Soil Environ 380 (2014) 101-115.

[38] J. Pett-Ridge, M.K. Firestone, Using stable isotopes to explore root-microbe-mineral interactions in soil, Rhizosphere 3 (2017) 244-253.
[39] A.M. Herrmann, K. Ritz, N. Nunan, P.L. Clode, J. Pett-Ridge, M.R. Kilburn, D.V. Murphy, A.G. O'Donnell, E.A. Stockdale, Nano-scale secondary ion mass spectrometry—a new analytical tool in biogeochemistry and soil ecology: a review article, Soil Biology and Biochemistry 39(8) (2007) 1835-1850.
[40] C. Kaiser, M.R. Kilburn, P.L. Clode, L. Fuchslueger, M. Koranda, J.B. Cliff, Z.M. Solaiman, D.V. Murphy, Exploring the transfer of recent plant photosynthates to soil microbes: mycorrhizal pathway vs direct root exudation, New Phytologist 205(4) (2015) 1537-51.
[41] P. Marschner, D. Crowley, Z. Rengel, Rhizosphere interactions between microorganisms and plants govern iron and phosphorus acquisition along the root axis - model and research methods, Soil Biol Biochem 43(5) (2011) 883-894.
[42] I.C. Grieve, D.A. Davidson, N.J. Ostle, P.M.C. Bruneau, A.E. Fallick, Spatial heterogeneity in the relocation of added 13C within the structure of an upland grassland soil, Soil Biology and Biochemistry 38(2) (2006) 229-234.
[43] P. Bruneau, N. Ostle, D.A. Davidson, I.C. Grieve, A.E. Fallick, Determination of rhizosphere 13C pulse signals in soil thin sections by laser ablation isotope ratio mass spectrometry, Rapid Commun Mass Sp 16(23) (2002) 2190-2194.
[44] E.H. Denis, P.D. Ilhardt, A.E. Tucker, N.L. Huggett, J.J. Rosnow, J.J. Moran, Spatially tracking carbon through the root-rhizosphere-soil system using laser ablation-IRMS, Journal of Plant Nutrition and Soil Science (2019).
[45] A. Rodionov, E. Lehndorff, C.C. Stremtan, W.A. Brand, H.-P. Konsigshoven, W. Amelung, Spatial micro-analysis of natural 13C/12C abundance in environmental samples using laser-ablation isotope-ratio-mass spectrometry, Anal Chem (2019).
[46] J.J. Moran, M.L. Alexander, A. Laskin, Soil Carbon: Compositional and Isotopic Analysis, in: R. Lal (Ed.), Encyclopedia of Soil Science, Third Edition, CRC Press, Boca Raton, FL, 2016, pp. 2073-2077.
[47] L. van Roij, A. Sluijs, J.J. Laks, G.J. Reichart, Stable carbon isotope analyses of ng quantities of particulate organic carbon (pollen) with laser ablation nano combustion gas chromatography isotope ratio mass spectrometry, Rapid Commun Mass Spectrom (2017).
[48] J.F. Kelly, R.L. Sams, T.A. Blake, M. Newburn, J. Moran, M.L. Alexander, H. Kreuzer, A capillary absorption spectrometer for stable carbon isotope ratio (C-13/C-12) analysis in very small samples, Rev Sci Instrum 83(2) (2012).
[49] J.M. Kriesel, C.N. Makarem, M.C. Phillips, J.J. Moran, M.L. Coleman, L.E. Christensen, J.F. Kelly, Versatile, ultra-low sample volume gas analyzer using a rapid, broad tuning ECQCL and a hollow fiber gas cell, Proc Spie 10210 (2017).
[50] J.A. Harrington, A Review of IR Transmitting, Hollow Waveguides, Fiber and Integrated Optics 19(3) (2000) 211-227.
[51] J.M. Kriesel, C.N. Makarem, A. Fahrland, J.J. Moran, T. Linley, J.F. Kelly, M. Razeghi, J.S. Lewis, G.A. Khodaparast, P. Khalili, Hollow fiber mid-IR spectrometer with UV laser ablation sampling for fine spatial resolution of isotope ratios in solids, Quantum Sensing and Nano Electronics and Photonics XVII, 2020.
[52] USDA-NRCS, Fact sheet for release of Cave-in-Rock switchgrass (*Panicum virgatum* L.), in: E.P.M.C. USDA-Natural Resources Convervation Service, Elsberry, MO, USA (Ed.) 2011.
[53] G.P. Robertson, S.K. Hamilton, Long-Term Ecological Research at the Kellogg Biological Station LTER site, in: S.K. Hamilton, J.E. Doll, G.P. Robertson (Eds.), The Ecology of Agricultural Lanscapes: Long-Term Research on the Path to Sustainability, Oxford University Press, New York, 2015, pp. 1-32.
[54] J.J. Moran, M.K. Newburn, M.L. Alexander, R.L. Sams, J.F. Kelly, H.W. Kreuzer, Laser ablation isotope ratio mass spectrometry for enhanced sensitivity and spatial resolution in stable isotope analysis, Rapid Commun Mass Sp 25(9) (2011) 1282-1290.
[55] C.M. Bledt, J.A. Harrington, J.M. Kriesel, Loss and modal properties of Ag/AgI hollow glass waveguides, Applied Optics 51(16) (2012) 3114-3119.

[56] I.E. Gordon, L.S. Rothman, C. Hill, R.V. Kochanov, Y. Tan, P.F. Bernath, M. Birk, V. Boudon, A. Campargue, K.V. Chance, B.J. Drouin, J.M. Flaud, R.R. Gamache, J.T. Hodges, D. Jacquemart, V.I. Perevalov, A. Perrin, K.P. Shine, M.A.H. Smith, J. Tennyson, G.C. Toon, H. Tran, V.G. Tyuterev, A. Barbe, A.G. Csaszar, V.M. Devi, T. Furtenbacher, J.J. Harrison, J.M. Hartmann, A. Jolly, T.J. Johnson, T. Karman, I. Kleiner, A.A. Kyuberis, J. Loos, O.M. Lyulin, S.T. Massie, S.N. Mikhailenko, N. Moazzen-Ahmadi, H.S.P. Muller, O.V. Naumenko, A.V. Nikitin, O.L. Polyansky, M. Rey, M. Rotger, S.W. Sharpe, K. Sung, E. Starikova, S.A. Tashkun, J. Vander Auwera, G. Wagner, J. Wilzewski, P. Wcislo, S. Yu, E.J. Zak, The HITRAN2016 molecular spectroscopic database, J Quant Spectrosc Ra 203 (2017) 3-69.
[57] N. Bilyera, I. Kuzyakova, A. Guber, B.S. Razavi, Y. Kuzyakov, How "hot" are hotspots: Statistically localizing the high-activity areas on soil and rhizosphere images, Rhizosphere 16 (2020).
[58] J.J. Moran, C.G. Doll, H.C. Bernstein, R.S. Renslow, A.B. Cory, J.R. Hutchison, S.R. Lindemann, J.K. Fredrickson, Spatially tracking C-13-labelled substrate (bicarbonate) accumulation in microbial communities using laser ablation isotope ratio mass spectrometry, Env Microbiol Rep 6(6) (2014) 786-791.
[59] R. Starke, N. Jehmlich, F. Bastida, Using proteins to study how microbes contribute to soil ecosystem services: The current state and future perspectives of soil metaproteomics, J Proteomics 198 (2019) 50-58.
[60] A. Macabuhay, B. Arsova, R. Walker, A. Johnson, M. Watt, U. Roessner, Modulators or facilitators? Roles of lipids in plant root-microbe interactions, Trends Plant Sci 27(2) (2022) 180-190.
[61] N.M. van Dam, H.J. Bouwmeester, Metabolomics in the Rhizosphere: Tapping into Belowground Chemical Communication, Trends Plant Sci 21(3) (2016) 256-265.
[62] R.A. White, A. Rivas-Ubach, M.I. Borkum, M. Koberl, A. Bilbao, S.M. Colby, D.W. Hoyt, K. Bingol, Y.M. Kim, J.P. Wendler, K.K. Hixson, C. Jansson, The state of rhizospheric science in the era of multi-omics: A practical guide to omics technologies, Rhizosphere 3 (2017) 212-221.
[63] P. Tian, B.S. Razavi, X.C. Zhang, Q.K. Wang, E. Blagodatskaya, Microbial growth and enzyme kinetics in rhizosphere hotspots are modulated by soil organics and nutrient availability, Soil Biol Biochem 141 (2020).
[64] K. Adhikari, A.E. Hartemink, Linking soils to ecosystem services - A global review, Geoderma 262 (2016) 101-111.
[65] J. Pausch, Y. Kuzyakov, Carbon input by roots into the soil: Quantification of rhizodeposition from root to ecosystem scale, Global Change Biology 24(1) (2018) 1-12.
[66] S.H. Villarino, P. Pinto, R.B. Jackson, G. Pineiro, Plant rhizodeposition: A key factor for soil organic matter formation in stable fractions, Sci Adv 7(16) (2021).

Supplemental Figure 1: Rhizobox used for plant growth. We cultured switchgrass seedlings in rhizoboxes packed with soil from the Kellogg Biological Station (Hickory Corners, MI, USA). The sides of the box could be removed to reveal root growth and distribution through the soil. Following isotopic labeling of the system (by incubation under $^{13}CO_2$) we removed the side panel from the box and harvested ½" diameter round subsamples which were selected to include roots and associated rhizosphere.

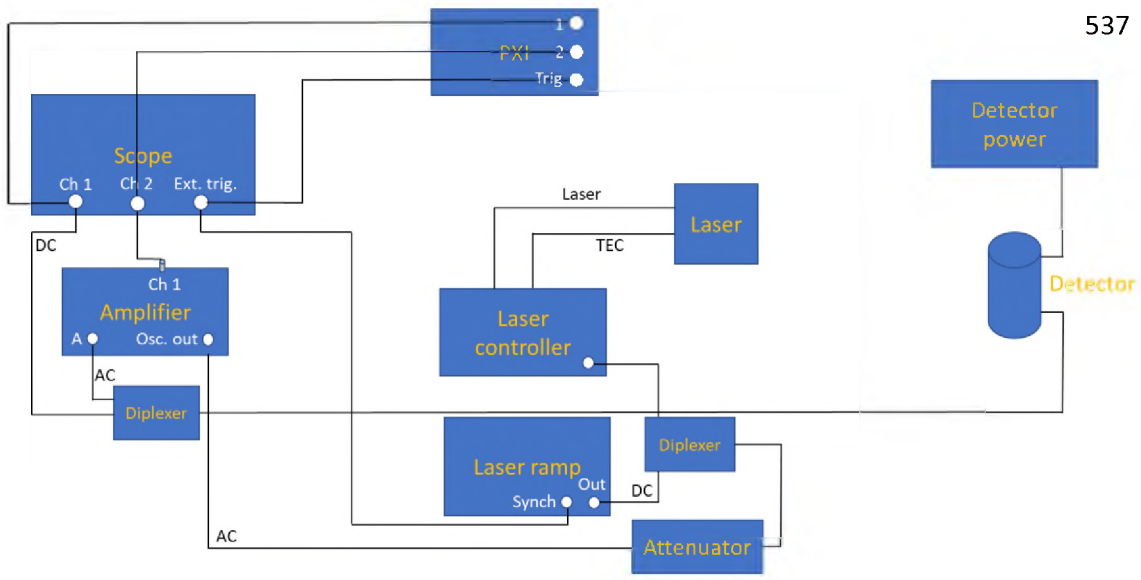

538 **Supplemental Figure 2**: Electronic components used for CAS analysis.

Measurement approach	LA-IRMS			LA-CAS		
Sample matrix	root	rhizosphere/soil	fishing line	root	rhizosphere/soil	fishing line
Ablation diameter (µm)	50	50	50	25	25	25
Number of ablation shots	1 - 10	80 - 100	8	1 - 2	30	2 - 3
Final sampling pit width (µm)	50	100	50	25	25	25
Ablation frequency (Hz)	20	20	20	20	20	20
Approximate power (mJ)	≤ 9	≤ 9	≤ 9	≤ 9	≤ 9	≤ 9

Declaration of interests

☒ The authors declare that they have no known competing financial interests or personal relationships that could have appeared to influence the work reported in this paper.

☐The authors declare the following financial interests/personal relationships which may be considered as potential competing interests: